A New Derivation of GRB Jet Opening Angles from the Prompt Gamma-Ray Emission

Adam Goldstein[1], Robert D. Preece[1], Michael S. Briggs[1], Alexander J. van der Horst[2], Sheila McBreen[3], Chryssa Kouveliotou[4], Valerie Connaughton[1], William S. Paciesas[1], Charles A. Meegan[2], P. N. Bhat[1], Elisabetta Bissaldi[5], J. Michael Burgess[1], Vandiver Chaplin[1], Roland Diehl[5], Gerald J. Fishman[4], Gerard Fitzpatrick[3], Suzanne Foley[5], Melissa Gibby[6], Misty Giles[6], Jochen Greiner[5], David Gruber[5], Sylvain Guiriec[1], Andreas von Kienlin[5], Marc Kippen[7], Arne Rau[5], Dave Tierney[3], and Colleen Wilson-Hodge[4]

Received _____; accepted _____

[1]University of Alabama in Huntsville, 320 Sparkman Drive, Huntsville, AL 35899, USA

[2]Universities Space Research Association, 320 Sparkman Drive, Huntsville, AL 35899, USA

[3]University College, Dublin, Belfield, Stillorgan Road, Dublin 4, Ireland

[4]Space Science Office, VP62, NASA/Marshall Space Flight Center, Huntsville, AL 35812, USA

[5]Max-Planck-Institut für extraterrestrische Physik (Giessenbachstrasse 1, 85748 Garching, Germany)

[6]Jacobs Technology

[7]Los Alamos National Laboratory, PO Box 1663, Los Alamos, NM 87545, USA

ABSTRACT

The jet opening angle of gamma-ray bursts (GRBs) is an important parameter for determining the characteristics of the progenitor, and the information contained in the opening angle gives insight into the relativistic outflow and the total energy that is contained in the burst. Unfortunately, a confident inference of the jet opening angle usually requires broadband measurement of the afterglow of the GRB, from the X-ray down to the radio and from minutes to days after the prompt gamma-ray emission, which may be difficult to obtain. For this reason, very few of all detected GRBs have constrained jet angles. We present an alternative approach to derive jet opening angles from the prompt emission of the GRB, given that the GRB has a measurable E_{peak} and fluence, and which does not require any afterglow measurements. We present the distribution of derived jet opening angles for the first two years of the Fermi Gamma-ray Burst Monitor (GBM) operation, and we compare a number of our derived opening angles to the reported opening angles using the traditional afterglow method. We derive the collimation-corrected gamma-ray energy, E_γ, for GRBs with redshift and find that some of the GRBs in our sample are inconsistent with a proto-magnetar progenitor. Finally, we show that the use of the derived jet opening angles results in a tighter correlation between the rest-frame E_{peak} and E_γ than has previously been presented, which places long GRBs and short GRBs onto one empirical power law.

Subject headings: gamma rays: bursts — methods: data analysis

1. Introduction

The Gamma-Ray Burst Monitor (GBM) onboard the Fermi Gamma-Ray Space Telescope has detected over 500 GRBs in its first 2 years of operation. A forthcoming catalog (Goldstein et al. 2011) contains time-integrated and time-resolved spectra for nearly all bursts during this time frame. With 12 sodium iodide (NaI) detectors and two bismuth germanate (BGO) detectors, GBM covers a wide energy band from 8 keV up to 40 MeV with roughly 2000 square centimeters of total detector surface area (Meegan et al. 2009). This energy range effectively samples the prompt emission of GRBs and allows for rapid all-sky triggering and monitoring. To gather information about the GRB afterglow properties, redshift, and jet opening angle, other instruments are required. Since GBM can only localize a burst to 4 degree accuracy including systematic uncertainties (Briggs et al. 2011), a simultaneous detection with *Swift* is usually required to derive a precise location for follow-up observations. *Swift* comprises a Burst Alert Telescope (BAT), an X-Ray Telescope (XRT) and an Ultraviolet-Optical Telescope (UVOT) (Barthelmy et al. 2005). The *Swift* prompt energy coverage extends from 20 – 150 keV, which does not allow for a comprehensive study of the higher energy prompt emission of GRBs which normally peaks at a few hundred keV. Therefore, it is obvious that the synergy between GBM and *Swift* results in a better understanding of this phenomenon. However, since there are relatively few GRBs that have been simultaneously detected by *Swift* and GBM, we are motivated to extend the ability to determine intrinsic properties of GRBs, such as jet opening angles and energetics, to the GBM observations of the prompt emission alone, using *Swift* afterglow studies for calibration.

Current GRB theories assume that the explosions are collimated rather than isotropic, because otherwise the extreme energy outflow in gamma-rays during the prompt emission would eliminate many of the viable stellar mass progenitor models (Rhoads 1997; Sari et al.

1999). In fact, Rhoads (1997) and Sari et al. (1999) proposed observable, achromatic 'jet' breaks in the broadband afterglow light curves of GRBs to distinguish the jet collimation opening angle before such breaks were discovered (Granot & Ramirez-Ruiz 2010). It is now widely accepted that GRBs are collimated, yet few well-constrained jet angles have been unambiguously identified. Further, nearly all estimated jet opening angles have been for the long soft class of GRBs, while there are no constrained estimates for the short hard class (Kouveliotou et al. 1993), most likely because short GRB afterglows are fainter and are thus less likely to be monitored long enough to detect a break (Gehrels et al. 2008; Kann & Klose 2008). In addition, precise locations are required and time must be requested of various observatories over a broad spectral range to study the late-time afterglow from minutes to days after the prompt emission. Several observational constraints and effects can hamper the identification of jet breaks such as gaps in temporal and spectral coverage and the presence of optical bumps in the light curve and X-ray flares. Even if a jet break is detected, an assumption of the density of the circumburst medium is required (Sari et al. 1999; Chevalier & Li 2000), and so a certain amount of uncertainty is inherent in the calculation of the jet opening angle.

Once determined, jet opening angles can lead to an estimate of the total energy release in gamma-rays. If the redshift and the prompt emission fluence of the GRB are also known, the collimation-corrected energy release at the source will provide the total energy budget of the GRB. These results constrain progenitor models and provide an estimate of the bulk Lorentz factor of the ejecta (Granot & Ramirez-Ruiz 2010). In addition, a more reliable and robust study of cosmology would be possible if a large number of collimation-corrected energies were known (Bloom et al. 2003). Such studies are currently incomplete due to small statistics. For example, out of nearly 500 GRBs detected by GBM through July 2010, only 30 have observed redshifts from the simultaneous detection by *Swift* , and of these 30 GRBs only 8 have inferred jet opening angles from afterglow studies. The importance of

GRBs to cosmology has recently become very clear with the detection of bursts out to a z of 8.2 (Tanvir et al. 2009), making these events among the farthest detected in the observable Universe. Many authors have studied the spectral properties such as the peak luminosity; isotropic energy release in gamma-rays, E_{iso}; the peak energy of the GRB power density spectrum, E_{peak} (Mallozzi et al. 1995; Koshut et al. 1996; Lloyd et al. 2000; Amati et al. 2002; Bloom et al. 2003; Ghirlanda et al. 2004; Yonetoku et al. 2004; Firmani et al. 2006). The purpose of this paper is to show that we can provide an alternative to the afterglow lightcurve monitoring method by deriving jet opening angles from the prompt emission of GRBs. We then utilize the opening angles to estimate the collimation-corrected energy release in gamma-rays, E_γ, and show that there is a tight correlation between E_{peak} and E_γ. Section 2 describes the data sample and section 3 consists of our data analysis methods and results. Finally, we discuss the cosmological consequences and implications for progenitors of our study in section 4.

2. Data Sample

Two data samples were used in this study. The 'redshift' sample consists of 30 bursts from the first 2-year GBM catalog as well as 3 more bursts in the third year (GRB 100724A, 100814A, and 100816A). All other bursts (without redshift) were chosen by selecting events from the entire GBM catalog from the first two years (Goldstein et al. 2011) according to the following data selection cuts. First, the spectral data were retrieved from fits performed with the standard GBM spectral fitting program, RMfit. Two models were investigated: the Band GRB function (Band et al. 1993), which comprises two power laws smoothly joined at a break energy that is unique to each burst; and a 'Comptonized' model, which is a power law with a high-energy exponential cutoff. Both models were parametrized with the E_{peak} parameter, which is the energy at which peak power production is measured.

Both models well describe nearly 80% of all GRB spectra, though the both functions are purely empirical and are not derived from physical quantities. The fitting statistic used in RMfit is the Castor C-statistic, a modification of the Cash statistic (Cash 1979). For each burst, a model comparison was performed by calculating the change in likelihood between the two models and determining the corresponding chi-square distribution for 1 degree of freedom (as the Comptonized model has one more degree of freedom and is nested within the Band model). We choose a change in likelihood of 6 units per one degree of freedom, which has a chance probability of about .01, as a threshold for a model to be preferred. The values of interest in our study are E_{peak} and fluence, so a data cut was performed on the error in E_{peak} and the fluence. Only those bursts that had an error of 40% or less of the mean value of the quantity of interest were allowed into the sample. This was done to ensure the integrity of our data sample and the following analysis.

3. Data Analysis and Results

3.1. $\mathbf{E_{peak}}$ & Fluence

To begin, we investigate a new discriminator between two types of bursts (long and short), the E_{peak}/Fluence energy ratio (Goldstein et al. 2010), which was discovered using BATSE data. This ratio provides a measure of spectral hardness similar to that found by Kouveliotou et al. (1993), but it is independent of redshift in energy and is directly related to the luminosity distance. Shown in Figure 1 is the distribution of 382 GRBs from the GBM spectral catalog (Goldstein et al. 2011). Using the preliminary duration results from the upcoming GBM GRB Catalog (Paciesas et al. 2011), the figure strongly supports the original claim by Goldstein et al. (2010) and shows the distribution separated into long bursts and short bursts, and a correspondence has been found between the energy ratio and the observed duration estimate of the bursts.

In an attempt to relate the rest-frame E_{peak} with the total energy release in gamma-rays, Amati et al. (2002) discovered a correlation between the rest-frame E_{peak} and E_{iso}, the bolometric energy release in gamma-rays assuming isotropic emission. The correlation is highly susceptible to scatter and outliers, and may be a result of selection effects due to detector trigger and spectral criteria (Lloyd-Ronning & Ramirez-Ruiz 2002; Friedman & Bloom 2005; Nakar & Piran 2005; Band & Preece 2005). Ghirlanda et al. (2004) found a similar correlation using E_γ, the collimation-corrected energy release. The so-called Ghirlanda relation contains less scatter and fewer outliers, but requires an additional piece of information, the jet opening angle. Both of these correlations require the redshift of the GRB, yet previous papers (Nakar & Piran 2005; Band & Preece 2005) have devised a way to test the correlations with GRBs that have no observed redshift. We adopt this test to show in Figure 2 the lower limits of the Amati and Ghirlanda relations in the E_{peak}–Fluence plane, and we find that very few bursts ($\sim 18\%$) can follow the Amati relation, though all GBM bursts may be valid for the Ghirlanda relation. More importantly, we plot the long and short bursts separately for GBM and we find that most long bursts are clustered between the Amati and Ghirlanda lower limits, while most of the short bursts are linearly dispersed along the Ghirlanda lower limit. We assume a beaming factor of unity for the Ghirlanda relation in the Figure 2, indicating that the opening jet angle is 90 degrees, which is consistent with previous findings from BATSE (Goldstein et al. 2010). Interestingly, if we decrease the beaming factor (and thus the jet opening angle), the Ghirlanda lower limit moves towards the bulk of long bursts, and eventually all short bursts will violate the Ghirlanda lower limit. This gives support to the findings that long bursts have a dispersion of jet angles from small angles on the order of a degree up to 50 degrees (Frail et al. 2001; Nakar 2007; Panaitescu & Kumar 2002) and short bursts have larger average jet opening angles of 40-90 degrees, as is supported theoretically by Livio & Waxman (1999) and observationally by Watson et al. (2006).

3.2. Jet Opening Angles

As indicated, the combination of the E_{peak}–Fluence plane and the Ghirlanda lower limit admit derived jet opening angles for GRBs, since the Ghirlanda lower limit appears to describe a true cutoff in the E_{peak}–Fluence plane that is consistent among multiple instruments. We can solve the lower limit from Ghirlanda's best fit equation (Ghirlanda et al. 2004), which was calibrated with GRBs that had well-constrained jet opening angles, in terms of the beaming fraction, observed E_{peak}, and fluence (see Band & Preece (2005); Goldstein et al. (2010)). Using this tool, we can derive jet opening angles for a large number of bursts with constrained E_{peak} values and fluences. In Table 1 we show the reported jet opening angles for bursts from afterglow studies in our redshift sample and compare them to our derived jet opening angles. There was no data selection cut based on parameter error due to the small sample size, therefore Table 1 contains a few angles with large error bars. In a number of cases, two different angles were inferred for a single burst, sometimes in conflict with each other. It should be noted that Cenko et al. (2010) used radio observations to constrain the physical parameters in their sample, while radio measurements were not used by McBreen et al. (2010) or Rau et al. (2010). Using only the four bursts with well-constrained reported jet angles, the Spearman's rank correlation coefficient for the reported angles and the derived angles is 0.8 with a probability of 0.2 that the two quantities are not correlated given the null hypothesis. Encouraged by the good agreement (within errors) between our estimates and the reported values of jet opening angles, we can now determine the jet angle for bursts without a measured redshift. In Figure 3 we show the jet opening angles for 382 GRBs from the GBM spectral catalog that have E_{peak} and fluence errors less than 40% of the mean value, resulting in an error in jet opening angle of no more than 40% for 85% of our calculated values. The distribution for long GRBs is extremely similar to the inferred range of opening angles from afterglow studies (2-50 degrees), while the short GRBs cluster closer to 90 degrees.

3.3. Energetics & Correlations

We now proceed to explore the actual Amati and Ghirlanda relations with our data. In Figure 4 we show the rest-frame E_{peak} versus the estimated isotropic energy release, E_{iso} for the GBM redshift sample. This is a direct test of the E_{peak}–E_{iso} relations with bursts of known redshift, however we can use the derived upper limits of the relations to help constrain the correlations. From Figure 4, we find the long bursts are loosely dispersed along the Amati relation (Amati et al. 2002), yet a number of long bursts are situated several sigma above the Amati upper limit (dotted line), which implies that if the bursts follow the Amati relation, their redshifts would be imaginary numbers. Interestingly, the Ghirlanda relation (Ghirlanda et al. 2004)well describes the linear dispersion of short hard GRBs if a jet opening angle of 90 degrees is assumed. This lends credence to the idea that short bursts are near isotropic bursters (Livio & Waxman 1999; Watson et al. 2006).

Using our derived jet opening angles, we can show that there is a correlation between the rest-frame E_{peak} and the total energy release in gamma-rays after correcting for collimation, E_γ, which is tantamount to a luminosity-distance relation. In previous attempts at such a relation, Amati et al. (2002) studied E_{iso}, which would seem to define a total energy budget for the explosion, but obtained a much looser correlation, and was unable to apply the relation to short GRBs. Ghirlanda et al. (2004), however, studied inferred E_γ obtained from jet opening angles deduced from broadband afterglow observations of a few GRBs and found a tighter relation than Amati et al. (2002); they were still unable to fit short GRBs into the relation. Figure 5 shows the distribution of E_γ from the derived jet opening angles, which is wider than previous estimates (Frail et al. 2001; Panaitescu & Kumar 2002) at 5 orders of magnitude and appears to peak near 1×10^{51} erg, although this may be due to a larger sample size compared to those previous studies. For a few bursts in the redshift sample, E_γ surpasses the total energy limit for a proto-magnetar,

which is a few$\times 10^{52}$ erg (Metzger et al. 2010) and a number of other bursts would require a very high efficiency to have viable magnetar progenitors, therefore according to our results, it is doubtful that a number of GRBs in our redshift sample originate from magnetar progenitors. The energy budget for neutron star mergers is in the range of a few$\times 10^{53}$ erg (Woosley 1993), while theoretically collapsars could emit up to 10^{54} erg (Woosley 1993; Paczynski 1998) at extremely high efficiency, which is compatible with our results.

Using the derived E_γ obtained from the clear cutoff in the E_{peak}–Fluence plane, Figure 6 shows the new relation and provides a much tighter correlation than either of the two previous relations. It also shows that short GRBs are clearly not outliers after correction for the much wider beaming angle. We present the best fit power law as

$$E_{peak}^{rest} = (589 \pm 18 \text{ keV}) \left(\frac{\mathrm{E}_\gamma}{10^{51} \text{ erg}} \right)^{0.49 \pm 0.01} \quad (1)$$

where the empirical power law was fitted to both coordinates. The power law normalization is of the same order as that found by Ghirlanda et al. (2004) (480 keV), but the power law index is very similar to that found by Amati et al. (2002) (0.52). The Spearman's rank correlation coefficient for E_{peak} and E_γ is 0.91 with a probability of 3×10^{-13} that the two quantities are not correlated given the null hypothesis. The calculated scatter around the best fit power law is about 0.1 dex for bursts with redshift $\sim 0.5 \leq z \leq 8.2$ and covering over 4 orders of magnitude in energy.

4. Conclusions

We have confirmed the E_{peak}/Fluence energy ratio results for GBM bursts, and have shown how they can be related to two different classes of GRBs. Most likely the larger of the two distributions belongs primarily to the long class of bursts typically associated with low-metallicity core-collapse supernovae, while the smaller mode belongs to the

short class which is believed to be associated with neutron star-neutron star and neutron star-black hole mergers. The distribution of the energy ratio provides information for the determination of the rest-frame energetics, as can be seen in more detail when plotted in the E_{peak}–Fluence plane. The hard spectral cutoff in this plane is apparent for all BATSE and GBM bursts, despite the fact that these were detected with two different instruments with different sensitivities and different band passes. From this we can infer the cutoff is most likely not detector dependent, and using only physical observables, we can derive one of the most important parameters of GRBs, the jet opening angle, and given an observed redshift, calculate E_γ.

Previously, the jet opening angle was only inferred for a handful of bursts for which X-ray, optical, and radio measurements of the afterglow were available (Sari et al. 1999). Even if these measurements were available, very few bursts have discernible jet breaks that denote the moment at which the relativistic ejecta slow down to the point that the observed relativistic beaming angle is the same as the actual beaming angle of the outflow (Granot & Ramirez-Ruiz 2010). Ghirlanda et al. (2005) derived jet opening angles without afterglow measurements, although their derivation required the bursts to be described by the Ghirlanda relation and relied on the lag-luminosity relationship (Norris et al. 2000) to derive pseudo-redshifts, yielding an ensemble distribution of jet opening angles. From this, they postulated that bursts with softer E_{peak} have larger opening angles than bursts with harder E_{peak}. By traditional classification of GRBs (Kouveliotou et al. 1993), the interpretation is that short hard GRBs would have smaller opening angles than long soft GRBs. This is, in general, contradictory to our findings. To contrast, our results show that we can reproduce jet opening angles for individual GRBs that can be spectrally analyzed with prompt emission alone and does not require the estimation of pseudo-redshifts. Our resulting distribution of opening angles also agrees with a current theoretical model that the beamed outflow at the rotational poles of the progenitor is produced by the rotational

angular momentum, as well as the configuration of the magnetic field (Livio & Waxman 1999). In this model, the degree of collimation is related to the ratio of radius of the compact object to the radius of the accretion disk. In the case of a collapsar, the radius of the central object is much smaller than the radius of the disk, resulting in a tightly collimated beam, while a merger model results in much less collimation since the radius of the accretion disk is on the order of the radius of the central object. Due to the much larger opening angles, observations of jet breaks for most short hard GRBs as well as some from the long soft class are unlikely since the estimated jet break times will be on the order of several months (Sari et al. 1999).

Applying the jet opening angle to the redshift sample, we can estimate the entire energy outflow in gamma-rays. From our results, we can rule out a proto-magnetar progenitor for a few long GRBs (080916C, 080810, 090323, 090519, and 090902B) as well as a short GRB (090510). When we compare this energy budget for each GRB to the E_{peak}, we find a clear correlation between the energy of peak power production and the total energy output in gamma-rays. One major distinction of our relation shows that both classes of GRBs can be described by the same power law fit, which has not been previously shown. The uncertainties of our calculations include geometric effects, as GRBs are likely seen slightly off- axis from the center of the jet, and this error propagates through to the calculation of E_{γ}. These uncertainties will likely be small for long bursts with small opening angles, due to the small possible displacement of the viewing angle relative to the jet opening angle. This relationship may potentially be exploited to extrapolate a rough redshift distribution for GRBs without redshift estimates, although a larger sample of GRBs with measured redshift is desired to confirm the existence of such a relation between E_{peak} and E_{γ}.

5. Acknowledgements

A.G. acknowledges the support of the Graduate Student Researchers Program funded by NASA as well as the support and recommendations of the GBM Science & Support Team.

REFERENCES

Amati, L., et al. 2002, A&A, 390, 81

Band, D. L., et al. 1993, ApJ, 413, 281

Band, D. L. & Preece, R. D. 2005, ApJ, 627, 319

Barthelmy, S. D., et al. 2005, Space Science Reviews, 120, 143

Bloom, J. S., Frail, D. A., & Kulkarni, S. R. 2003, ApJ, 594, 674

Briggs, M. S., et al. 2011, in prep

Cash, W. 1979, ApJ, 228, 939

Cenko, S.B., et al. 2010, submitted to ApJ, arxiv: 1004.2900v2

Chandra, P., et al. 2010, ApJ, 712, L31

Chevalier, R. A. & Li, Z. 2000, ApJ, 536, 195

Firmani, C., Ghisellini, G., Avila-Reese, V., & Ghirlanda, G. 2006, MNRAS, 370, 185

Frail, D. A. 2001, ApJ, 562, L55

Friedman, A. S., & Bloom, J. S. 2005, ApJ, 627, 1

Gehrels, N., et al. 2008, ApJ, 689, 1161

Ghirlanda, G., Ghisellini, G., & Lazzati, D. 2004, ApJ, 616, 331

Ghirlanda, G., Ghisellini, G., & Firmani, C. 2005, MNRAS, 361, L10

Goldstein, A., Preece, R. D., & Briggs, M. S. 2010, ApJ, 721, 1329

Goldstein, A., et al., in prep

Granot J. & Ramirez-Ruiz, E. 2010, arXiv:1012.5101v1 [astro-ph.HE]

Greiner, J., et al. 2009, A&A, 498, 89

Kaneko, Y., Preece, R. D., Briggs, M. S., Paciesas, W. S., Meegan, C. A., & Band, D. L. 2006, ApJS, 166, 298

Kann, D. A., & Klose, S. 2008, AIP Conf. Proc. 1000, Gamma-Ray Bursts 2007: Proceedings of the Santa Fe Conference, ed. M. Galassi, D. Palmer, $ E. Fenimore, 293

Koshut, T., Mallozzi, R. S., Horack, J., Paciesas, W. S., Kouveliotou, C., & Rutledge, R. 1996, AIP Conf. Proc. 384, Gamma-ray bursts: 3rd Huntsville Symposium, ed. C. Kouveliotou, M. S. Briggs, & G. J. Fishman, 446

Kouveliotou, C., Meegan, C. A., Fishman, G. J., Bhat, N. P., Briggs, M. S., Koshut, T. M., Paciesas, W. S., & Pendleton, G. N. 1993, ApJ, 413, L101

Livio, M., & Waxman, E. 1999, ApJ, 538, 187

Lloyd, N. M., Petrosian, V., & Mallozzi, R. S. 2000, ApJ, 534, 227

Lloyd-Ronning, N. M., & Ramirez-Ruiz, E. 2002, ApJ, 576, 101

Mallozzi, R. S., Paciesas, W. S., Pendleton, G. N., Briggs, M. S., Preece, R. D., Meegan, C. A., & Fishman, G. J. 1995, A&A, 454, 597

McBreen, S., et al. 2010, A&A, 516, A71

Meegan, C. A., et al. 2009, ApJ, 702, 791

Metzger, B. D., Giannios, D., Thompson, T. A., Bucciantini, N., & Quataert, E. 2010, arXiv:1012.0001v1 [astro-ph.HE]

Nakar, E., & Piran, T. 2005, MNRAS, 360, L73

Nakar, E. 2007, Physics Reports, 442, 166

Norris, J. P., Marani, G. F. & Bonnell, J. T., 2000, ApJ, 534, 248

Paciesas, W. S., et al. 2011, in prep.

Paczynski, B. 1998, ApJ, 494, L45

Page, K. L, et al. 2009, MNRAS, 400, 134

Panaitescu, A., & Kumar, P. 2002, ApJ, 571, 779

Rau, A., et al. 2010, ApJ, 720, 862

Rhoads, J.E. 1997, ApJ, 487, L1

Sari R., Piran, T., & Halpern, J. P. 1999, ApJ, 524, L43

Tanvir, N. et al. 2009, GCN Circular 9219

Watson, B., Hjorth, J., Jakobsson, P., Xu, D., Fynbo, J. P. U, Sollerman, J., Thöne, C. C., & Pedersen, K. 2006, A&A, 454, L123

Woosley, S. E. 1993, ApJ, 405, 273

Yonetoku, D., et al. 2004, ApJ, 609, 935

Yuan, Fang. *Chasing the Brightest Cosmic Explosions with ROTSE-III* (Ph.D. diss). University of Michigan, 2010

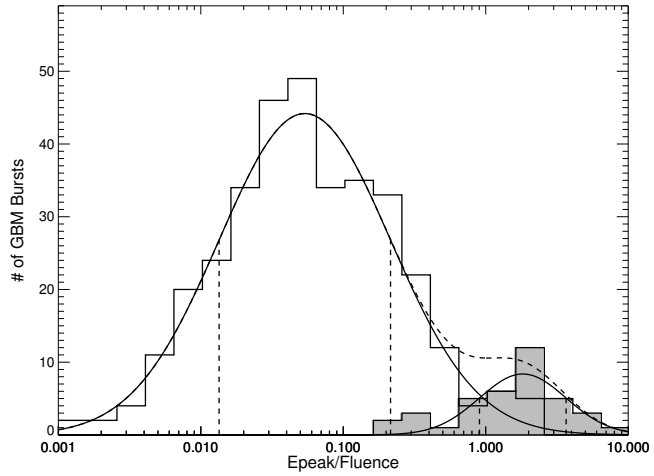

Fig. 1.— The E_{peak}/Fluence energy ratio for 344 long GRBs (white) and 38 short GRBs (gray). A fit was performed on the entire distribution and the χ^2 goodness-of-fit for the two lognormal functions is 12.2 for 14 degrees of freedom. Fitting a single lognormal function to the distribution results in a goodness-of-fit of 27.8 for 17 degrees of freedom. The change in χ^2 per degree of freedom results in a chance probability of 1×10^{-3} that the two lognormals are not preferred. The vertical dotted lines denote the 1-σ standard deviation of each lognormal.

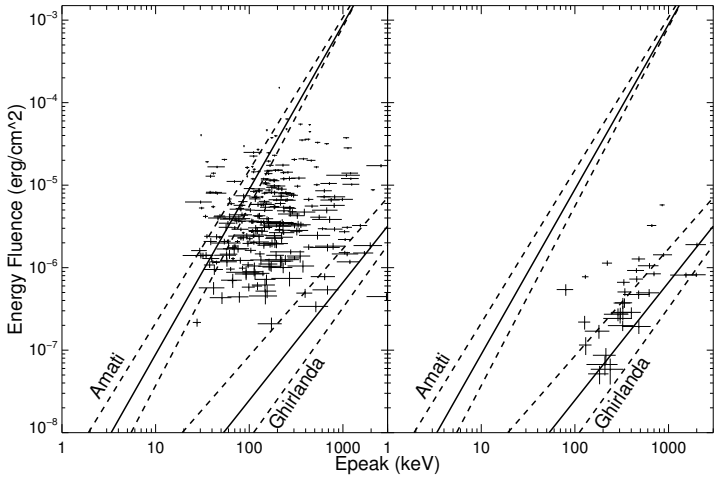

Fig. 2.— Plot of 382 GBM bursts in the E_{peak}-Fluence plane. The left side shows the 344 long GRBs and the right shows the 38 short. The plotted lines are the Amati and Ghirlanda upper limits, which in this plane become lower limits. From this we see that very few GRBs follow the Amati relation, since a majority of the bursts fall below the lower limit. The Ghirlanda lower limit, however, appears to be near a true lower bound. Therefore, the Ghirlanda limit can be shown to admit a large spread of mostly small jet opening angles for long bursts and mostly large opening angles for short bursts.

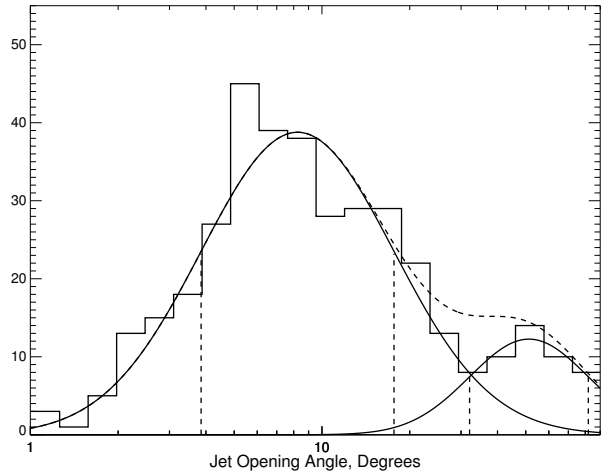

Fig. 3.— Distribution of derived jet opening angles for 382 GBM GRBs. The relative propagated errors for this plot do not exceed 0.40 for 85% of our sample, and 51% of our sample do not exceed a relative error of 0.1. The best fit lognormal functions have aχ^2 goodness-of-fit of 12.9 for 14 degrees of freedom. The mean value for the large distribution is ~ 8 degrees and the mean for the smaller distribution ~ 51 degrees. The vertical dotted lines show the 1-σ standard deviations of the respective distributions.

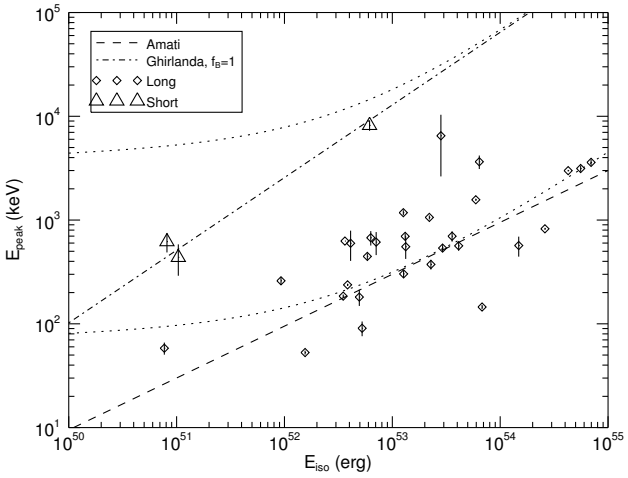

Fig. 4.— Plot of the E_{peak}–E_{iso} plane. The dotted lines denote the upper limits for the two well-noted correlations. Most long bursts cluster around the Amati line, but with a large dispersion. The short bursts are situated along the the Ghirlanda line with corresponding jet opening angle of 90 degrees.

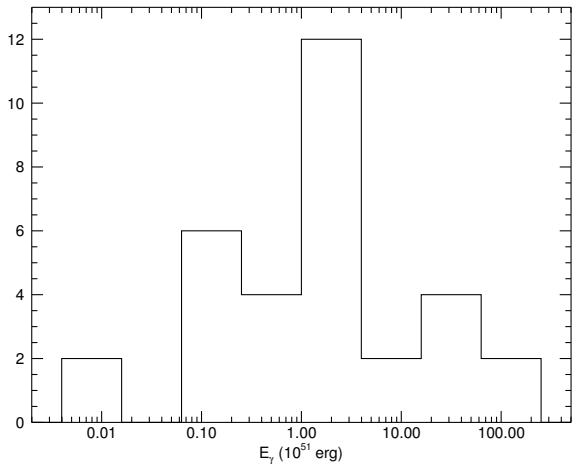

Fig. 5.— Plot of E_γ in units of 10^{51} erg from the redshift sample. The distribution covers about 5 orders of magnitude and peaks at 1×10^{51} erg. The bursts with E_γ greater than $\sim 3 \times 10^{52}$ are inconsistent with the magnetar progenitor model

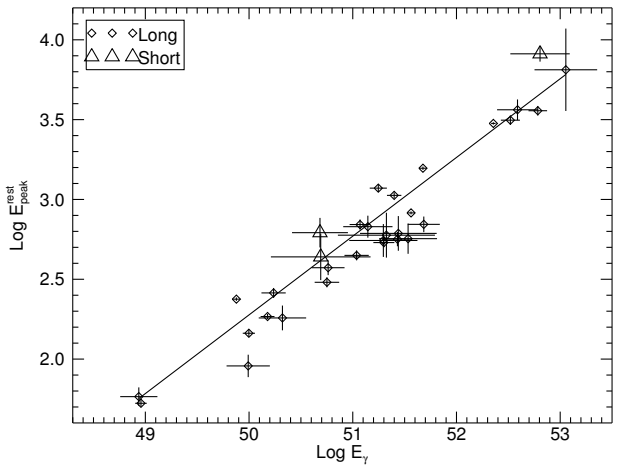

Fig. 6.— Plot of the rest-frame E_{peak} versus the total energy released in gamma-rays after correcting for collimation for the redshift sample. The best fit value of the normalization of the power law is 589 ± 18 kev and the best fit power law index is 0.49 ± 0.01. Note that the short GRBs follow the same correlation as long GRBs, which previous relations have been unable to show. The relation covers over 4 orders of magnitude in energy and spans GRBs from z of 0.5 up to 8.2.

Table 1. Comparison of Reported and Derived Jet Opening Angles

GRB	**Reported Angle(s)**	**Derived Angles**	**Reference**
080810	> 4.0 [a]	13.8 ± 6.4	Page et al. (2009)
080916C	> 6.1 [b]	5.2 ± 1.6	Greiner et al. (2009)
081008	> 2.1[b]	6.4 ± 4.0	Yuan (2010)
090323	< 2.1 [b]	4.3 ± 1.3	McBreen et al. (2010)
	$2.6^{+0.6}_{-0.1}$ [a]		Cenko et al. (2010)
090328	< 5.5 [b]	6.6 ± 11.9	McBreen et al. (2010)
	$5.2^{+1.4}_{-0.7}$ [a]		Cenko et al. (2010)
090423	> 12.0 [b]	11.0 ± 7.0	Chandra et al. (2010)
090902B	> 6.4 [b]	4.1 ± 0.6	McBreen et al. (2010)
	$3.4^{+0.4}_{-0.3}$ [b]		Cenko et al. (2010)
090926A	> 9.9 [b]	7.6 ± 2.6	Rau et al. (2010)
	$7.0^{+3.0}_{-1.0}$ [a]		Cenko et al. (2010)

[a]Wind Medium

[b]ISM